Many-body Fock sectors in Wick-Cutkosky model

Dae Sung Hwang [a,1] and V.A. Karmanov [b,*,2]

[a] *Department of Physics, Sejong University, Seoul 143–747, Korea*

[b] *Lebedev Physical Institute, Leninsky Prospekt 53, 119991 Moscow, Russia*

Abstract

In the model where two massive scalar particles interact by the ladder exchanges of massless scalar particles (Wick-Cutkosky model), we study in light-front dynamics the contributions of different Fock sectors (with increasing number of exchanged particles) to full normalization integral and electromagnetic form factor. It turns out that two-body sector always dominates. At small coupling constant $\alpha \ll 1$, its contribution is close to 100%. It decreases with increase of α. For maximal value $\alpha = 2\pi$, corresponding to the zero bound state mass, two-body sector contributes to the normalization integral 64%, whereas the three-body contribution is 26% and the sum of all higher contributions from four- to infinite-body sectors is 10%. Contributions to the form factor from different Fock sectors fall off faster for asymptotically large Q^2, when the number of particles in the Fock sectors becomes larger. So, asymptotic behavior of the form factor is determined by the two-body Fock sector.

Key words: Light-front dynamics, Fock sectors, electromagnetic form factors
PACS: 11.10.St, 11.15.Tk, 13.40.Gp

1 Introduction

In field theory, the decomposition of the state vector in the basis of free fields with given momenta results in the concept of relativistic wave function in momentum space. The latter is the coefficient of the decomposition – the Fock component. The state vector is described by an infinite set of the Fock components, corresponding to different numbers of particles.

* Corresponding author.
[1] e-mail: dshwang@sejong.ac.kr, dshwang@slac.stanford.edu
[2] e-mail: karmanov@sci.lebedev.ru, karmanov@lpsc.in2p3.fr

However, the models used in applications usually consider only few-body Fock components. The infinite set of the Fock components is truncated to one component only, with two or three quarks. The belief that a given Fock sector dominates is mainly based on intuitive expectations and "experimental evidences" rather than on field-theoretical analysis. Without this analysis a model remains to be phenomenological. Though one can perturbatively estimate the next Fock components (with one or even few extra particles), this says nothing about convergence of full Fock decomposition.

The difficulty to take into account the many-body sectors is caused by the fact that it is equivalent to solving a true field-theory problem. Important part of this problem – finding the Bethe-Salpeter (BS) function [1] – is solved in the Wick-Cutkosky model [2]. In this case the BS equation is reduced to the one-dimensional one which can be easily solved numerically for arbitrary coupling constant. In weak and strong coupling limits there are explicit analytical solutions. This allows us to use Wick-Cutkosky model for non-perturbative study the Fock decomposition.

In the Wick-Cutkosky model two spinless constituents with mass m interact by exchange by a massless scalar particle. Corresponding BS function is the "two-body" one in the sense that it depends on two four-dimensional particle coordinates. The term "two-body" here is rather slang than reflection of a real physical situation. It may be misleading. We emphasize that this *does not* mean that the "two-body" BS function describes a two-body system, i.e., a system with the state vector truncated to the two-body Fock component. On the contrary, the corresponding state vector contains infinite set of the Fock components with two massive constituents and $0, 1, 2, \ldots, \infty$ massless exchanged particles.

Fig. 1. Feynman ladder graph with two exchanges.

This can be explained as follows. In terms of the Feynman diagrams, the one-boson exchange kernel generates the ladder graphs only. One of these graphs, with two exchanges, is shown in Fig. 1. We will work in the light-front dynamics (LFD). In terms of the time-ordered graphs, in the light-front (LF) time, this Feynman diagram contributes to the two-, three- and four-body states (with two massive constituents and with zero, one and two exchanged

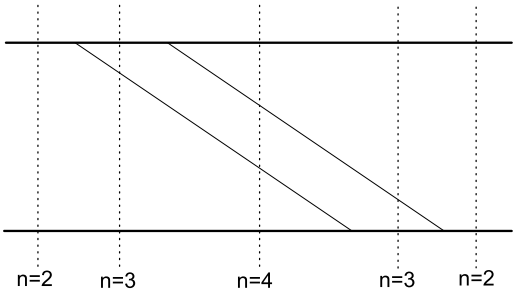

Fig. 2. One of six time-ordered ladder graphs, generated by the Feynman graph Fig. 1.

bosons). There are six such time-ordered graphs. One of these graphs is shown in Fig. 2. Since the BS equation deals with infinite series of ladder exchanges, it implicitly incorporates all the intermediate states with number of particles from two to infinity. The problem (solved in the present paper) is to "extract" from the BS solution the two-body contribution and total contribution of all other Fock components. Comparison of total contribution with the two-body one shows the contribution of the many-body sectors.

Because of the ladder kernel, the Wick-Cutkosky model is still approximate. All the exchange particles, emitted by one and the same boson, must be and absorbed by other one. The graphs with particles emitted by different bosons in the same intermediate state are generated by the cross Feynman box which is absent in the Wick-Cutkosky model. Self-energy graphs are absent too. In spite of these restrictions, the Wick-Cutkosky solution does contain in the state vector an infinite sum of many-body Fock components. Namely this property is most important for our work.

In Wick-Cutkosky model there are also some abnormal solutions which have no counterpart in the non-relativistic potential theory [2,3]. There was a discussion [3], whether they are physical ones or not. This is a separate problem, not related to our study. We deal with the normal solution. In non-relativistic limit the two-body Fock component, which only survives in the state vector of normal solution, turns into the usual ground state wave function in the Coulomb potential.

A truncated LF field theory was developed in [4]. Some estimations of the higher Fock sectors were done in [5]. Truncated LF Fock space decomposition was applied in [6] to nonperturbative study the large α QED. Recently, the Fock decomposition, incorporating first three Fock sectors, was used for nonperturbative renormalization in a scalar model [7] and, with two sectors, – in Yukawa model [8,9] and in gauge theory [9].

In the present paper, we study in the Wick-Cutkosky model the contribution of the many-body sectors in electromagnetic form factor and compare it with the two-body contribution. Besides, we calculate the contribution to the normalization integral of the two- and three-body states. Subtracting them from 1, we get contribution of all the states with $n \geq 4$. In this way we investigate the convergence of the Fock decomposition. Calculations are carried out nonperturbatively in full range of binding energy $0 \leq B \leq 2m$.

Plan of the paper is the following. In Section 2 we define the Fock decomposition (in the framework of LFD), and remind the definition of the BS function. In Section 4 the BS equation is solved. In addition to analytical solutions in limiting cases $M \to 2m$ and $M = 0$, found in [2], we find, for small α, next correction of the order of $\alpha \log \alpha$ and solve BS equation numerically for any α. In Section 5 the two-body contribution to the normalization integral and to the electromagnetic form factor is calculated for both small and large coupling constants. The form factor asymptotic at $Q^2 \to 0$ is obtained. In Section 6 the same is done for three-body contribution and in Section 7 for sum of all Fock sectors. Sect. 8 is devoted to numerical calculations for arbitrary coupling constant. Sect. 9 contains summary and discussion. Some technical details are given in Appendices A, B and C.

2 Fock decomposition and BS function

The state vector $|p\rangle$, eigenstate of full Hamiltonian, can be decomposed in terms of the eigenstates of free Hamiltonian. This results in natural formulation of the concept of a relativistic wave function in terms of the LF Fock expansion at fixed LF time, which is usually put to zero for a stationary state: $\omega{\cdot}x = 0$. The null four-vector ω ($\omega^2 = 0$) determines the orientation of the LF plane; the freedom to choose ω provides an explicitly covariant formulation of LF quantization [10]. The Fock decomposition has the form:

$$|p\rangle = \sum_{n\geq 2} \int \psi(k_1, \ldots, k_n, p, \omega\tau) \times \delta^{(4)}\left(\sum_j^n k_j - p - \omega\tau\right) 2(\omega{\cdot}p)\,\mathrm{d}\tau \prod_{i=1}^n \frac{\mathrm{d}^3 k_i}{(2\pi)^3 2\varepsilon_{k_i}} a^\dagger(\vec{k}_i)\,|0\rangle\,. \qquad (1)$$

Here $a^\dagger$ is the usual creation operator and $\varepsilon_{k_i} = \sqrt{m_i^2 + \vec{k}_i^{\,2}}$. All the four-momenta are on the corresponding mass shells: $k_j^2 = m_j^2$, $p^2 = M^2$, $(\omega\tau)^2 = 0$. In QCD, the set of LF Fock state wave functions $\psi(k_1, \ldots, k_n, p, \omega\tau)$ represents the ensemble of quark and gluon states possible when the hadron is intercepted at the light-front. In Wick-Cutkosky model this set represents

the states with two massive constituents $+0, 1, 2, \ldots$ massless exchange particles, forming two-, three-, four-body states, etc. The constituents are spinless and we consider the state $|p\rangle$ with total zero angular momentum. Therefore we omit the spin indices. The scalar variable τ controls the off-shell continuation of the wave function. From the point of view of kinematics, the four-momentum $\omega\tau$ can be considered on equal ground with the particle four-momenta $k_1, \ldots, k_n, p$. Being expressed through them (by squaring the equality $\sum_i^n k_i = p + \omega\tau$), τ reads: $\tau = (M_0^2 - M^2)/(2\omega{\cdot}p)$, where $M_0^2 = (\sum_i^n k_i)^2$.

For system with zero total angular momentum the wave functions ψ are the scalar functions and they depend on a set of scalar products of the four-momenta $k_1, \ldots, k_n, p, \omega\tau$ with each other. One should choose a set of $3n-4$ independent scalar products. A convenient way to choose these variables is the following. We define

$$x_i = \omega{\cdot}k_i/\omega{\cdot}p\ , \quad R_i = k_i - x_i p \tag{2}$$

and represent the spatial part of the four-vector $R_i = (R_{i0}, \vec{R}_i)$ as $\vec{R}_i = \vec{R}_{i\parallel} + \vec{R}_{i\perp}$, where $\vec{R}_{i\parallel}$ is parallel to $\vec{\omega}$ and $\vec{R}_{i\perp}$ is orthogonal to $\vec{\omega}$. In the standard version of LFD the difference $\sum_i k_i - p$ is non-zero for the minus component only. In covariant formulation this means: $\sum_i k_i = p + \omega\tau$. Therefore: $\sum_i \vec{R}_{i\perp} = 0$, $\sum_i x_i = 1$. Since $R_i{\cdot}\omega = R_{i0}\omega_0 - \vec{R}_{i\parallel}{\cdot}\vec{\omega} = 0$ by definition of R_i, it follows that $R_{i0} = |\vec{R}_{i\parallel}|$, and, hence, $\vec{R}_{i\perp}^2 = -R_i^2$ is Lorentz and rotation invariant. Similarly one can show that $\vec{R}_{i\perp}{\cdot}\vec{R}_{j\perp} = -R_i{\cdot}R_j$. Therefore the scalar products $\vec{R}_{i\perp}{\cdot}\vec{R}_{j\perp}$ are also Lorentz and rotation invariants. In terms of these variables the invariant energy $s \equiv M_0^2 = (\sum_i k_i)^2$ is given by

$$s = \sum_i \frac{\vec{R}_{i\perp}^2 + m_i^2}{x_i}. \tag{3}$$

The variables $\vec{R}_{i\perp}, x_i$ are analogous to the well-known variables in the infinite momentum frame [11].

The wave functions are parametrizd as: $\psi = \psi(\vec{R}_{1\perp}, x_1; \vec{R}_{2\perp}, x_2; \ldots; \vec{R}_{n\perp}, x_n)$ and should depend on x_i, $\vec{R}_{i\perp}^2$ and on $\vec{R}_{i\perp}{\cdot}\vec{R}_{j\perp}$. In terms of these variables, the integral in Eq. (1) is transformed as

$$\begin{aligned}
&\int \ldots \delta^{(4)}\left(\sum_j^n k_j - p - \omega\tau\right) 2(\omega{\cdot}p)\,\mathrm{d}\tau \prod_{i=1}^n \frac{\mathrm{d}^3 k_i}{(2\pi)^3 2\varepsilon_{k_i}} \\
&= \int \ldots 2\delta\left(\sum_j^n x_j - 1\right) \delta^{(2)}\left(\sum_j^n \vec{R}_{j\perp}\right) \prod_{i=1}^n \frac{\mathrm{d}^2 R_{i\perp}\,\mathrm{d}x_i}{(2\pi)^3 2x_i}.
\end{aligned}$$

The state vector (1) enters the definition of the BS function:

$$\Phi(x_1, x_2, p) = \langle 0| \, T(\varphi(x_1)\varphi(x_2)) \, |p\rangle \, . \tag{4}$$

Since the function $\Phi(x_1, x_2, p)$ depends on two four-dimensional coordinates x_1, x_2, one often refers to the function (4) as describing a two-body system. However, the state vector $|p\rangle$ is the full state vector. It contains all the Fock components, with the constituent numbers $n = 2, 3, 4, \ldots$. The operators $\varphi(x_1), \varphi(x_2)$ in (4) are the Heisenberg operators (of the massive field).

We need the BS function $\Phi(k, p)$ in the momentum space. It is related to (4) as follows:

$$\begin{aligned} &\Phi(x_1, x_2, p) = (2\pi)^{-3/2} \exp\Big(-ip\cdot(x_1 + x_2)/2\Big) \, \tilde{\Phi}(x, p), \\ &\Phi(k, p) = \int \tilde{\Phi}(x, p) \exp(ik\cdot x) \, \mathrm{d}^4 x, \end{aligned} \tag{5}$$

where $x = x_1 - x_2$ and $p = p_1 + p_2$ is the on-mass-shell momentum of the bound state ($p^2 = M^2$), p_1, p_2 are the off-shell momenta ($p_1^2 \neq p_2^2 \neq m^2$) and $k = (p_1 - p_2)/2$.

Knowing the BS function (5), we can extract from it the two-body component [10]:

$$\psi(\vec{R}_\perp, x) = \frac{(\omega\cdot k_1)(\omega\cdot k_2)}{\pi(\omega\cdot p)} \int\limits_{-\infty}^{+\infty} \Phi(k + \beta\omega, p) \, \mathrm{d}\beta. \tag{6}$$

This relation is independent of any model.

In the Wick-Cutkosky model, the BS function $\Phi(k, p)$ for the ground state with zero angular momentum $L = 0$ has the following integral representation [2,3]:

$$\Phi(k, p) = -\frac{i}{\sqrt{4\pi}} \int\limits_{-1}^{+1} \frac{g_M(z) \, \mathrm{d}z}{(m^2 - M^2/4 - k^2 - zp\cdot k - i\epsilon)^3} \, . \tag{7}$$

This representation is valid and exact for zero-mass exchange. The function $g_M(z)$ is determined by an integral equation [2,3] given below in Section 4. It is solved analytically in the limiting cases of asymptotically small and extremely large binding energy and numerically – for any binding energy.

Substituting (7) into (6), we find the two-body Fock component [12,13]:

$$\psi(\vec{R}_\perp, x) = \frac{x(1-x)g_M(1-2x)}{2\sqrt{\pi}\Big(\vec{R}_\perp^2 + m^2 - x(1-x)M^2\Big)^2} \ . \tag{8}$$

When we express electromagnetic form factor through the BS function, we do not make any truncation of the Fock space. We get sum of contributions of all the Fock components. On the other hand, having found the two-body component (8), we can calculate its contribution to form factor and to the full normalization integral. In addition, below we will calculate explicitly the three-body contribution. Comparison of full contribution with the two-body ones allows to find the many-body sector contribution, for arbitrary values of coupling constant. Comparison of two-body, three-body and full contributions allows to see, how the Fock decomposition converges. In the present paper we will realize this program.

We will use the BS function (7) and the LF two-body wave function (8) to calculate full form factor (and normalization integral) and two-body contribution to them. For these calculations we need to know the function $g_M(z)$.

3 Normalization condition for $g_M(z)$

Since the state vector $|p\rangle$ in definition (4) of the BS function is normalized, the BS function does not contain any arbitrary factors and, hence, is also properly normalized. The normalization factor cannot be found, of course, from the homogeneous BS equation, but is determined by a special normalization condition [3]. It is equivalent to the condition based on the charge conservation [3], which means that $F_{full}(0) = 1$. This condition determines the normalization of $g_M(z)$.

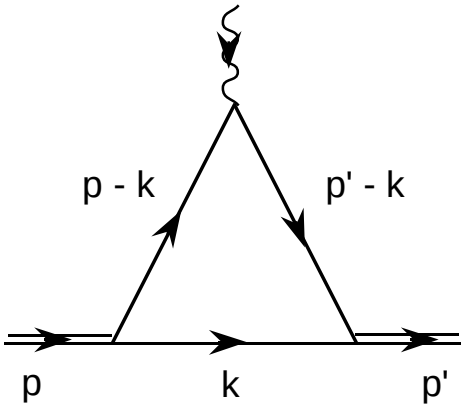

Fig. 3. Feynman diagram for the EM form factor.

The electromagnetic form factor $F_{full}(Q^2)$ ($Q^2 = -q^2 \geq 0$ and $q = p' - p$) is shown graphically in Fig. 3. The vertices at the left- and right-hand sides, being multiplied by the propagators, are the BS functions (5). Therefore the electromagnetic vertex is expressed in terms of the BS function as [10]

$$\begin{aligned} &(p+p')^\mu F_{full}(Q^2) \\ &= -i \int \frac{\mathrm{d}^4 k}{(2\pi)^4}\ (p+p'-2k)^\mu\ (m^2-k^2)\ \Phi\left(\frac{1}{2}p-k,p\right)\Phi\left(\frac{1}{2}p'-k,p'\right). \end{aligned} \tag{9}$$

We multiply both sides of (9) by $(p+p')_\mu$, insert (7) into (9), use the Feynman parametrization:

$$\frac{1}{a^3 b^3} = \int\limits_0^1 \frac{30u^2(1-u)^2\,\mathrm{d}u}{\Big(au+b(1-u)\Big)^6},$$

integrate (using Wick rotation) over four-vector k and replace the variables $z = 2x-1$, $z' = 2x'-1$. In this way, at $Q = 0$ we find the normalization condition:

$$\begin{aligned} F_{full}(0) = &-\frac{1}{2^5\pi^3}\int\limits_0^1 g_M(2x-1)\,\mathrm{d}x \int\limits_0^1 g_M(2x'-1)\,\mathrm{d}x' \\ &\times \int\limits_0^1 u^2\ (1-u)^2\,\mathrm{d}u\ \frac{\Big((6\xi-5)m^2+2\xi(1-\xi)M^2\Big)}{\Big(m^2-\xi(1-\xi)M^2\Big)^4} = 1, \end{aligned} \tag{10}$$

where $\xi = xu + x'(1-u)$.

4 Solution of Wick-Cutkosky equation

The integral equation for the function $g_M(z)$ for the ground state reads [2,3]:

$$g_M(z) = \frac{\alpha}{2\pi}\int\limits_{-1}^{1} K(z,z')g_M(z')\,\mathrm{d}z' \tag{11}$$

with the kernel:

$$K(z,z') = \frac{m^2}{m^2 - \frac{1}{4}(1-z'^2)M^2}\left[\frac{(1-z)}{(1-z')}\theta(z-z') + \frac{(1+z)}{(1+z')}\theta(z'-z)\right]. \tag{12}$$

Here $\alpha = g^2/(16\pi m^2)$ and g is the coupling constant in the interaction Hamiltonian $H^{int} = -g\varphi^2(x)\chi(x)$. In nonrelativistic limit the interaction is reduced

to the Coulomb potential $V(r) = -\frac{\alpha}{r}$. The function $g_M(z)$ is defined in the interval $-1 \leq z \leq 1$ and it is even: $g_M(-z) = g_M(z)$.

At small binding energy $B = 2m - M$, and, on the contrary, at extremely large binding energy equal to $2m$, the solutions $g_M(z)$ are found explicitly. At asymptotically small binding energy (corresponding to $\alpha \to 0$) it has the form [2]:

$$g_{M\to 2m}(z) = N_{M\to 2m}(1 - |z|) \tag{13}$$

and the binding energy is the non-relativistic one in the Coulomb potential: $B = \frac{m\alpha^2}{4}$. The normalization constant $N_{M\to 2m}$ is found by substituting $g_{M\to 2m}(z)$ into the normaization condition (10). Calculation gives:

$$N_{M\to 2m} = 8\sqrt{2}\pi\alpha^{5/2}m^3. \tag{14}$$

The higher Fock sectors are generated by extra exchanges which contain extra degrees of α. They are omitted in the solution (13). Therefore, to analyze the many-body contributions, we should take into account next $\sim \alpha$ correction to Eq. (13). To find it, we use the method of paper [14]. The correction contains both the terms $\sim \alpha$ and $\sim \alpha \log \alpha$. We keep the leading $\sim \alpha \log \alpha$ only. The details are given in Appendix A. The solution of Eq. (11) obtains the form:

$$g_M(z) = N\left[1 - |z| + \frac{\alpha}{2\pi}(1 + |z|)\log(z^2 + \alpha^2/4)\right]. \tag{15}$$

Corresponding binding energy $B = 2m - M$ is given by [14]:

$$B = \frac{m\alpha^2}{4} - \frac{m\alpha^3}{\pi}\log\frac{1}{\alpha}. \tag{16}$$

The normalization factor N in (15) (still found from the condition (10)) now reads:

$$N = 8\sqrt{2}\pi\alpha^{5/2}m^3\left[1 + \frac{5\alpha}{\pi}\log\alpha\right]. \tag{17}$$

In the opposite limiting case $B = 2m, M = 0$, which is achieved at $\alpha = 2\pi$, the solution has the form [2,3]:

$$g_{M=0}(z) = N_{M=0}(1 - z^2)\ . \tag{18}$$

The normalization coefficient reads:

$$N_{M=0} = 6\sqrt{30}\pi^{3/2}m^3. \tag{19}$$

The latter case is especially simply checked. We substitute Eq. (18) with the normalization (19) into Eq. (10) and find:

$$F_{full}(0) = 540 \int_0^1 u^2(1-u)^2 x(1-x)x'(1-x')(5-3x-3x')\ \mathrm{d}u\,\mathrm{d}x\,\mathrm{d}x' = 1.$$

This justifies the value (19).

The BS functions corresponding to the small and large binding energy solutions (13) and (18) are given explicitly in Appendix B.

For arbitrary bound state mass M we solve equation (11) numerically and find corresponding function $g_M(z)$ and coupling constant α. The interval $-1 \le z \le 1$ is split in 50 equal subintervals. In every subinterval the function $g_M(z)$ is represented by a sum of the quadratic spline functions. We substitute a given initial $g_M(z)$ in the right-hand side of (11), represent the result of numerical integration again through the spline functions and iterate. For $M \to 2m$ and $M \to 0$ we numerically reproduce the analytical solutions (13) and (18) correspondingly. The iterations converge very quickly. For example, for $M = 0$, even if we start iterations with the function (13), corresponding to the opposite limit $M \to 2m$, after a few iterations we reproduce the true solution (18). The accuracy of seven digits (for example) in the function $g_{M=0}(z)$ is achieved after 8 iterations.

In Fig. 4 the dependence of M on α is shown. In all the figures we use the units of m, i.e. we put $m = 1$. One can see that M turns into zero at $\alpha \approx 6.28$, that agrees with the analytical solution $\alpha(M = 0) = 2\pi$.

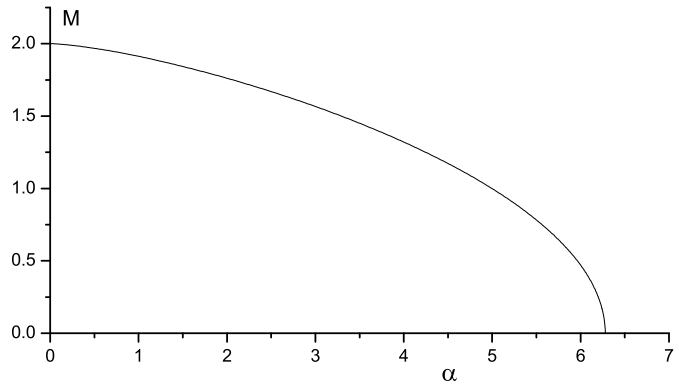

Fig. 4. Bound state mass M vs. coupling constant α. In all the figures we put $m = 1$.

To compare the form of the functions $g_M(z)$ vs. z for different M's, we, at first, normalize all $g_M(z)$'s by the condition $g_M(0) = 1$ and show them in Fig. 5 for

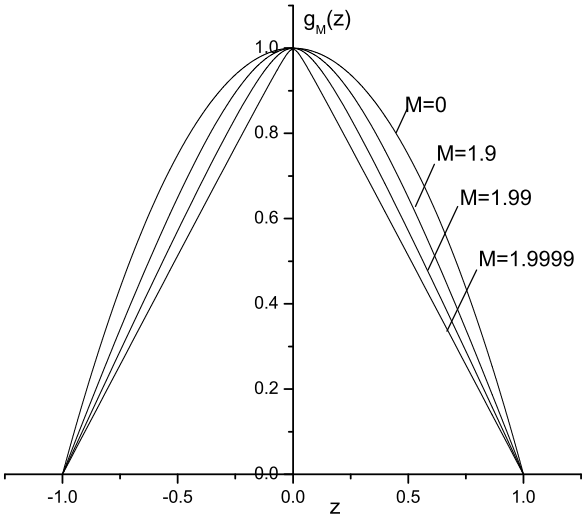

Fig. 5. Functions $g_M(z)$ normalized by $g_M(0) = 1$.

the values $M = 0,\ 1.9,\ 1.99,\ 1.9999$. It is seen that the form of $g_M(z)$ does not depend significantly on M. For very different values $M = 0$ and $M = 1.9$ the curves of $g_M(z)$ are rather close to each other. All the curves for $0 < M < 1.9$ are between these two curves. We emphasize that with the function $g_M(z)$ normalized by $g_M(0) = 1$ the form factor $F_{full}(0)$ is not normalized to 1.

The functions $g_M(z)$ normalized by the condition $F_{full}(0) = 1$, Eq. (10), are shown in Fig. 6 for the values $M = 0,\ 1,\ 1.5,\ 1.75,\ 1.9,\ 1.9999$. They strongly depend on M. This dependence comes mainly from the normalization factor. In the scale of Fig. 6 the function $g_M(z)$ at $M = 1.9999$ is indistinguishable from the z-axis.

Now we are in position to calculate form factors and two- and three-body contributions to the normalization integral.

5 Two-body contribution

5.1 Form factor

The two-body contribution $F_{2b}(Q^2)$ to form factor $F_{full}(Q^2)$ is shown graphically in Fig. 7. This diagram corresponds to the time-ordered (in the LF time) graph technique. The latter exists in a few versions [11,10,15], giving equivalent results. Dealing with the scalar particles, we will use the Weinberg rules [11] (given in Appendix C). Though the expression for two-body form factor in

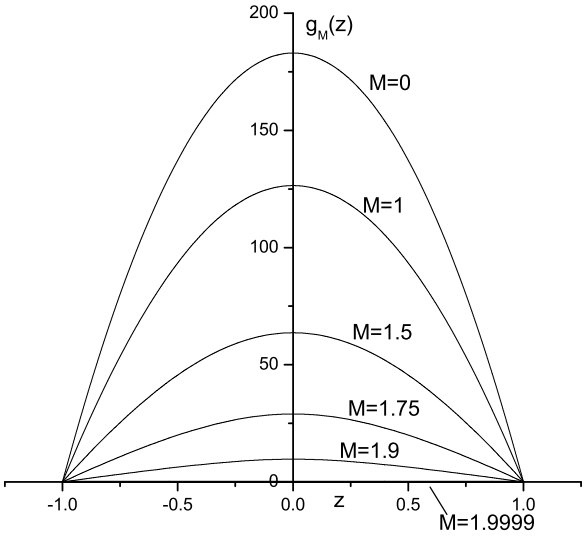

Fig. 6. Functions $g_M(z)$ normalized by $F_{full}(0) = 1$.

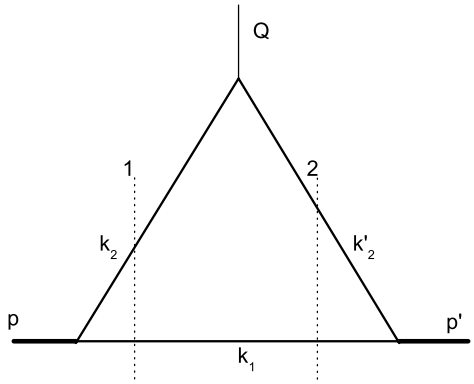

Fig. 7. LF diagram for the two-body contribution to the EM form factor.

terms of an overlap of the LF wave functions is well-known [10,15,16,17,18,19], we derive it in Appendix C. Form factor reads:

$$F_{2b}(Q^2) = \frac{1}{(2\pi)^3} \int \psi(\vec{R}_{1\perp}, x_1)\psi(\vec{R}_{1\perp} - x_1\vec{Q}_\perp, x_1)\frac{\mathrm{d}^2 R_{1\perp}\,\mathrm{d}x_1}{2x_1(1-x_1)}, \qquad (20)$$

where $\vec{Q}_\perp^2 = Q^2$. Substituting in (20) the wave function $\psi(\vec{R}_\perp, x)$ determined by Eq. (8) and combining two $\vec{R}_{1\perp}$-dependent denominators by means of the formula

$$\frac{1}{a^2 b^2} = \int\limits_0^1 \frac{6u(1-u)\,\mathrm{d}u}{\Big(au + b(1-u)\Big)^4},$$

we can easily integrate over $\vec{R}_{1\perp}$:

$$F_{2b}(Q^2) = \frac{1}{2^5\,\pi^3} \int\limits_0^1 \int\limits_0^1 \frac{x(1-x)\; g_M^2(2x-1)\,\mathrm{d}x\; u(1-u)\,\mathrm{d}u}{\Big(u(1-u)x^2Q^2 + m^2 - x(1-x)M^2\Big)^3}\;. \tag{21}$$

Calculating then the integral over u, we finally obtain:

$$F_{2b}(Q^2) = \frac{1}{2^5\pi^3 Q^6} \int\limits_0^1 \left[4\gamma(1+\gamma)\log\frac{\sqrt{1+4\gamma}+1}{\sqrt{1+4\gamma}-1} + (1-2\gamma)\sqrt{1+4\gamma}\right] \times \frac{(1-x)g_M^2(2x-1)\,\mathrm{d}x}{x^5\gamma(1+4\gamma)^{5/2}}, \tag{22}$$

where

$$\gamma = \frac{m^2 - x(1-x)M^2}{x^2Q^2}.$$

5.2 Normalization integral

5.2.1 Small binding energy ($M \to 2m$)

The two-body contribution to the normalization integral is found from (21) or (21):

$$N_2 = F_{2b}(0) = \frac{1}{192\,\pi^3} \int\limits_0^1 \frac{x(1-x)\; g_M^2(2x-1)\,\mathrm{d}x}{\Big(m^2 - x(1-x)M^2\Big)^3}\;. \tag{23}$$

In the limit of asymptotically small binding energy ($\alpha \to 0$) we should substitute in (23) the function $g_{M\to 2m}(z)$, Eq. (13), and keep the leading term only (which now is $\sim \alpha^0 = 1$). In this case we obtain a trivial result:

$$N_2 = 1.$$

We see that the normalization integral is saturated by the two-body Fock sector. The higher Fock sectors are generated by graphs with extra exchanges, each of them containing extra degree of coupling constant α. Their contributions are out of the leading α-term, which was only kept in the function $g_{M\to 2m}(z)$. They are neglected in the limit $\alpha \to 0$, that results in $N_2 = 1$.

Now we calculate N_2 in next to the leading order, taking into account the correction $\sim \alpha\log\alpha$. For this aim, we substitute in the integral (23) the solution

(15). Calculating the integral (23) and keeping the terms $\sim \alpha \log \alpha$, we obtain:

$$N_2 = 1 - \frac{2\alpha}{\pi} \log \frac{1}{\alpha}. \tag{24}$$

Hence, for the contribution of the higher Fock sectors with $n \geq 3$: $N_{n\geq 3} = 1 - N_2$, we find:

$$N_{n\geq 3} = \frac{2\alpha}{\pi} \log \frac{1}{\alpha}. \tag{25}$$

Below, in Section 6.2, we will compare Eq. (25) for $N_{n\geq 3} = N_3 + N_4 + N_5 + \ldots$ with the three-body contribution N_3.

5.2.2 Extremely large binding energy ($M \to 0$)

In this case we should substitute in (23) the function $g_{M=0}(z)$, Eq. (18), and put $M = 0$. This gives:

$$N_2 = F_{2b}(0) = 90 \int\limits_0^1 x^3 (1-x)^3 \, \mathrm{d}x = \frac{9}{14} \approx 64\%. \tag{26}$$

The value of many-body contribution $N_{n\geq 3} = 1 - N_2$ at $M = 0$ ($B = 2m$):

$$N_{n\geq 3} = 1 - N_2 = \sum_{n=3}^{\infty} N_n = 5/14 \approx 36\% \tag{27}$$

is the maximal value in the model. For $M = 0$ the sum $\sum_{n=3}^{\infty} N_n$ over the many-body Fock sectors contains increasing degrees of huge coupling constant $\alpha = 2\pi$. However it still converges (to the value 5/14).

5.3 Asymptotic at $Q^2 \to \infty$

5.3.1 Small binding energy ($M \to 2m$)

In the limit $M \to 2m$, form factor is obtained by substituting in (22) the solution (13) for $g_{M\to 2m}(z)$. It was calculated, by a different method, in [20]. The asymptotic formula reads:

$$F_{2b}^{asymp}(Q^2) \approx \frac{16\alpha^4 m^4}{Q^4} \left[1 + \frac{\alpha}{2\pi} \log \left(\frac{Q^2}{m^2} \right) \right]. \tag{28}$$

The limit $M \to 2m$ corresponds, for massless exchange kernel, to $\alpha \to 0$. As explained above, in the leading α order the contribution of higher Fock sectors is neglected. Therefore in this approximation the two-body contribution coincides with the full one. They coincide not only in asymptotic, but everywhere.

5.3.2 Extremely large binding energy ($M \to 0$)

Substituting in (21) the expression (18) for $g_{M=0}(z)$ and making replacement of variable $u(1-u) = v$, we find at $M = 0$:

$$F_{2b}(Q^2) = 1080m^6 \int\limits_0^1 x^3(1-x)^3 \,\mathrm{d}x \int\limits_0^{1/4} \frac{v \,\mathrm{d}v}{(m^2 + Q^2 v x^2)^3 \sqrt{1-4v}}. \tag{29}$$

Form factor (29) is calculated explicitly:

$$\begin{aligned} F_{2b}(Q^2) = \frac{180m^4}{(Q^2)^3} \Bigg[& 60m^2 - 7Q^2 + 36m^2 \log^2 \frac{\sqrt{4m^2+Q^2} + \sqrt{Q^2}}{2m} \\ & + 3(Q^2 - 20m^2)\sqrt{1 + \frac{4m^2}{Q^2}} \log \frac{\sqrt{4m^2+Q^2} + \sqrt{Q^2}}{2m} \Bigg]. \end{aligned} \tag{30}$$

At $Q \to \infty$ we find:

$$F_{2b}^{asymp}(Q^2) = \frac{270m^4}{Q^4} \left[\log\left(\frac{Q^2}{m^2}\right) - \frac{14}{3} \right]. \tag{31}$$

It is instructive to compare $F_{2b}^{asymp}(Q^2)$ with full form factor and with the three-body one. This will be done below.

6 Three-body contributions

6.1 Form factor

Comparison of two-body contribution $F_{2b}(Q^2)$ with full form factor $F_{full}(Q^2)$ (made below analytically for asymptotic domain and numerically for any Q^2) shows the total contribution to form factor of the higher Fock sectors with $n = 3, 4, 5, \ldots$. In order to see the convergence of the Fock decomposition, we calculate in this section the first term of this sum, i.e., the three-body contributions. The diagrams are shown in figs. 8 (a) and (b).

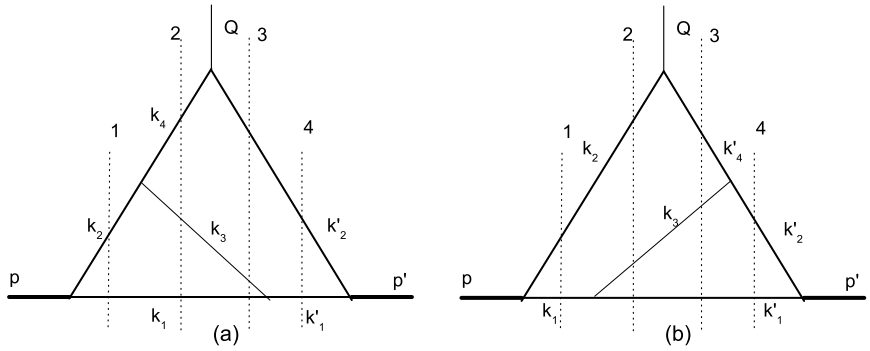

Fig. 8. Three-body contributions to form factor.

Figures 9 (a) and (b) also represent the three-body intermediate states. The graph Fig. 9 (a) incorporates self-energy, whereas the graph Fig. 9 (b) can be interpreted as a correction to the constituent form factor. However, in the ladder approximation, they do not contribute and therefore are omitted. There are no other three-body states.

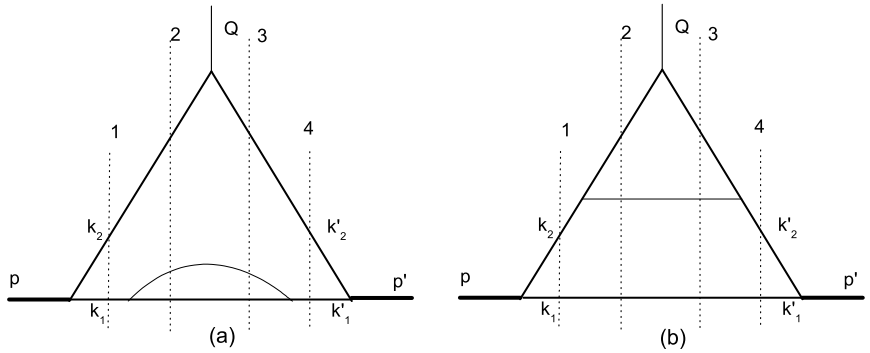

Fig. 9. Three-body states which do not contribute to form factor in the ladder model.

The three-body form factor is calculated in Appendix C.2. The diagrams (a) and (b) in Fig. 8 give equal contributions. Therefore we take expression for diagram Fig. 8 (a) and multiply it by 2. The result has the form:

$$F_{3b}(Q^2) = \frac{\alpha m^2}{2\pi^5} \int \frac{\psi(\vec{R}_{1\perp}, x_1)\, \psi(\vec{R}'_{1\perp}, x'_1)}{(s_2^{(a)} - M^2)\,(s_3^{(a)} - M^2)}\, \frac{\theta(x'_1 - x_1)}{(x'_1 - x_1)}$$

$$\times \frac{\mathrm{d}^2 R_{1\perp}\,\mathrm{d}x_1}{2x_1(1-x_1)}\;\frac{\mathrm{d}^2 R'_{1\perp}\,\mathrm{d}x'_1}{2x'_1(1-x'_1)}. \tag{32}$$

The variables $s_2^{(a)}$, $s_3^{(a)}$ are the energies squared in the intermediate states 2 and 3 in Fig. 8 (a). They are expressed in terms of the integration variables $\vec{R}_\perp$, $\vec{R'}_\perp$ and also $\vec{Q}_\perp$ (see Appendix C.2):

$$s_2^{(a)} = \frac{\vec{R}_{1\perp}^2 + m^2}{x_1} + \frac{(\vec{R'}_{1\perp} - \vec{R}_{1\perp} + x'_1\vec{Q}_\perp)^2}{x'_1 - x_1} + \frac{(\vec{R'}_{1\perp} + x'_1\vec{Q}_\perp)^2 + m^2}{1-x'_1}, \tag{33}$$

$$s_3^{(a)} = \frac{(\vec{R}_{1\perp} - x_1\vec{Q}_\perp)^2 + m^2}{x_1} + \frac{(\vec{R'}_{1\perp} - \vec{R}_{1\perp} + x_1\vec{Q}_\perp)^2}{x'_1 - x_1} + \frac{\vec{R'}_{1\perp}^{\,2} + m^2}{1-x'_1}. \tag{34}$$

We emphasize that in contrast to the two-body form factor (20), the variable $\vec{R'}_{1\perp}$ in (32) is not expressed through $\vec{R}_{1\perp}$ and $\vec{Q}_\perp$. Both $\vec{R}_\perp$ and $\vec{R'}_\perp$ are independent integration variables.

6.2 Normalization integral

Three-body contribution N_3 to full normalization integral is simply $N_3 = F_{3b}(0)$, that with Eq. (32) gives:

$$N_3 = \frac{\alpha m^2}{2\pi^5}\int \frac{\psi(\vec{R}_{1\perp}, x_1)\;\psi(\vec{R'}_{1\perp}, x'_1)}{(s_a - M^2)^2}\;\frac{\theta(x'_1 - x_1)}{(x'_1 - x_1)} \times \frac{\mathrm{d}^2 R_{1\perp}\,\mathrm{d}x_1}{2x_1(1-x_1)}\;\frac{\mathrm{d}^2 R'_{1\perp}\,\mathrm{d}x'_1}{2x'_1(1-x'_1)}, \tag{35}$$

where

$$s_a = \frac{\vec{R}_{1\perp}^2 + m^2}{x_1} + \frac{(\vec{R'}_{1\perp} - \vec{R}_{1\perp})^2}{x'_1 - x_1} + \frac{\vec{R'}_{1\perp}^{\,2} + m^2}{1-x'_1}. \tag{36}$$

In the leading $\alpha\log\alpha$ order N_3 is calculated analytically in Appendix C.2.2. The result is the following:

$$N_3 = \frac{2\alpha}{\pi}\log\frac{1}{\alpha}, \tag{37}$$

i.e., it coincides with $N_{n\geq 3}$, Eq. (25). It is natural, since the difference between $N_{n\geq 3}$ and N_3 is due to the higher Fock sectors $N_{n\geq 4}$, which contain extra degrees of α omitted in the present calculation.

The numerical calculations of N_3 vs. M will be given in Section 8. At $M = 0$ we get: $N_3 = 0.257$. This illustrates the convergence of the Fock decomposition at $\alpha = 2\pi$: $N_2 \approx 64\%$, $N_3 \approx 26\%$, $N_4 + N_5 + \ldots \approx 10\%$.

6.2.1 Asymptotic at $Q^2 \to \infty$

As discussed above, at asymptotically small binding energy only two-body contribution survives. Therefore we consider here the case of extremely large binding energy only. Since $\psi(\vec{R}_\perp, x)$ at large $R_\perp$ decreases like $\sim 1/R_\perp^4$ (see Eq. (8)), the integral (32) well converges. Therefore we can take the limit $Q^2 \to \infty$ directly in the integrand. We put $\alpha = 2\pi$, corresponding to $M = 0$. For the Q-dependent factor in (32) we find:

$$\lim_{Q^2\to\infty} \frac{1}{(s_2^{(a)} - M^2)(s_3^{(a)} - M^2)} = \frac{(1-x')(x'-x)^2}{x(1-x)x'^2} \, \frac{1}{Q^4}.$$

Then the integral:

$$F_{3b}^{asymp}(Q^2) = \frac{1}{Q^4} \, \frac{m^2}{4\pi^4} \int\limits_0^1 \mathrm{d}x' \int\limits_0^{x'} \mathrm{d}x \frac{(x'-x)}{x^2(1-x)^2x'^4} \times\psi_{M=0}(\vec{R'}_\perp, x') \, \mathrm{d}^2R'_\perp \psi_{M=0}(\vec{R}_\perp, x) \, \mathrm{d}^2R_\perp$$

with the wave function $\psi_{M=0}$ given by Eq. (B.5) is easily calculated and we get:

$$F_{3b}^{asymp}(Q^2) = \frac{180m^4}{Q^4}. \tag{38}$$

7 Full contribution

7.1 Form factor

The contribution of all Fock components is incorporated by the form factor $F_{full}(Q^2)$ in Eq. (9). Its calculation does not differ from the normalization integral explained in Section 3. The results is:

$$F_{full}(Q^2) = -\frac{1}{2^5\pi^3} \int\limits_0^1 g_M(2x-1) \, \mathrm{d}x \int\limits_0^1 g_M(2x'-1) \, \mathrm{d}x' \int\limits_0^1 u^2 \, (1-u)^2$$

$$\times \frac{\Big(xx'u(1-u)Q^2 + (6\xi-5)m^2 + 2\xi(1-\xi)M^2\Big)}{\Big(xx'u(1-u)Q^2 + m^2 - \xi(1-\xi)M^2\Big)^4}\,\mathrm{d}u, \qquad (39)$$

where $\xi = xu + x'(1-u)$. At $Q = 0$ form factor (39) turns into the normalization integral (10).

7.2 Asymptotic at $Q^2 \to \infty$

As explained in Section 5.3.1, in the limit of asymptotically small binding energy the higher Fock sector contribution disappears. Therefore the full form factor $F_{full}(Q^2)$ coincides with the two-body one $F_{2b}(Q^2)$, which has asymptotic given by Eq. (28).

We calculate asymptotic of $F_{full}(Q^2)$ in the opposite case of extremely large binding energy. For this aim we substitute in (39) the function $g_{M=0}(z)$ from (18) and make the replacement $v = u(1-u)$. This gives:

$$F_{full}(Q^2) = 540m^6 \int\limits_0^{1/4} \frac{v^2\,\mathrm{d}v}{\sqrt{\frac{1}{4}-v}} \int\limits_0^1 x(1-x)\,\mathrm{d}x \int\limits_0^1 x'(1-x')\,\mathrm{d}x' \times \frac{\Big(m^2(5-3x-3x') - Q^2xx'v\Big)}{(m^2+Q^2vxx')^4}. \qquad (40)$$

The integrals over x and x' are calculated analytically: [3]

$$F_{full}(Q^2) = -\frac{540m^4}{Q^8} \int\limits_0^{1/4} \frac{\mathrm{d}v}{v^2\sqrt{1-4v}} \Big[2Q^2v(3m^2+Q^2v) - (m^2+Q^2v)(6m^2+Q^2v)\log\left(1+\frac{Q^2v}{m^2}\right) - 2m^2Q^2v\mathrm{Li}_2\left(-\frac{Q^2v}{m^2}\right)\Big].$$

Now we take the limit $Q^2 \to \infty$ and therefore keep in the integrand the leading term $\propto Q^4$. We obtain:

[3] $\mathrm{Li}_2(z) \equiv \mathrm{Polylog}(2,z)$ is a special function dilogarithm:

$$\mathrm{Li}_2(z) = \int\limits_z^0 \log(1-t)\frac{dt}{t}.$$

The leading terms of $\mathrm{Li}_2(-z)$ at $z \to \infty$ are $\mathrm{Li}_2(-z) \approx -\frac{1}{2}\log^2(z+1) - \frac{\pi^2}{6}$.

$$F_{full}(Q^2) \approx -\frac{540m^4}{Q^4} \int\limits_0^{1/4} \frac{\mathrm{d}v}{\sqrt{1-4v}} \left[2 - \log\left(1 + \frac{Q^2 v}{m^2}\right)\right].$$

It is also calculated analytically. Taking again the leading term at $Q^2 \to \infty$, we find the asymptotic:

$$F_{full}^{asymp}(Q^2) \approx \frac{270m^4}{Q^4} \left[\log\left(\frac{Q^2}{m^2}\right) - 4 \right]. \tag{41}$$

Comparing (41) with Eq. (31) for F_{2b}, we see that at $Q \to \infty$ the leading terms $\frac{270m^4}{Q^4} \log\left(\frac{Q^2}{m^2}\right)$ of F_{full} and F_{2b} , exactly coincide with each other. This means that asymptotic of F_{full} is dominated by F_{2b} and the many-body contributions decrease faster with increase of Q^2 than the two-body one.

Comparing Eqs. (31), (38) and (41), we find the relation

$$F_{full}^{asymp}(Q^2) = F_{2b}^{asymp}(Q^2) + F_{3b}^{asymp}(Q^2) \tag{42}$$

valid for the terms $\sim 1/Q^4$. We see that the term $\sim \frac{1}{Q^4} \log \frac{Q^2}{m^2}$ in F_{full}^{asymp} comes from F_{2b}^{asymp} and the difference between F_{full}^{asymp} and F_{2b}^{asymp} of the order of $\sim \frac{1}{Q^4}$ results from $F_{3b}^{asymp}(Q^2)$. The corrections to Eq. (42) result from the higher contributions F_{4b}, F_{5b}, etc. Since they are absent in (42) in the order $\frac{1}{Q^4}$, they decrease more rapidly than $\frac{1}{Q^4}$. This shows a hierarchy of asymptotic form factors: $F_{2b} > F_{3b} > F_{4b} > \ldots$. This also indicates a good convergence of contributions of the Fock components with increasing particle numbers, a least, in asymptotic. In Section 8 we will calculate numerically the different contributions to the normalization integral (i.e., take the opposite, $Q^2 = 0$ limit) and also find good convergence.

7.3 Arbitrary binding energy

The momentum transfer Q^2 enters the equation (39) for form factors F_{full} in the combination $xx'Q^2$, and in the equation (21) for F_{2b} as x^2Q^2. Therefore, the form factors at $Q^2 \to \infty$ are determined by the integration domain near $x, x' \to 0$ and, hence, by behavior of the function $g_M(z = 2x - 1)$ at binding point $z = -1$. As shown in Section 4, at $z \to -1$ the function $g_M(z)$ linearly tends to zero: $g_M(z \to -1) \sim (z + 1)$, independently of the value of M. Therefore, the asymptotic $F_{full}(Q^2) \sim F_{2b}(Q^2) \sim \frac{1}{Q^2} \log(\frac{Q^2}{m^2})$ is expected for any M. This is natural, since this asymptotic is valid in both limiting cases $M = 0$ and $M \approx 2m$.

To check that, we represent $g_M(z)$ as: $g_M(z) = (z^2-1)f(z)$, where the factor (z^2-1) provides zeroes at $z = \pm 1$ and $f(z)$ is an even function of z which can be decomposed near $z = 0$ as: $f(z) = c_0 + c_2 z^2 + c_4 z^4 + \ldots$. When we take the zero degree in this decomposition, i.e. the term c_0 only, we come back to the case $g_M(z) \propto (1-z^2)$, considered in the case $M = 0$, and therefore for arbitrary binding energy we obtain the asymptotic $F_{full}(Q^2) \sim F_{2b}(Q^2) \sim \frac{1}{Q^2}\log(\frac{Q^2}{m^2})$ found for $M = 0$. Other terms of decomposition result in the factor $z^{2m}z'^{2n} = (2x-1)^{2n}(2x'-1)^{2n}$ which does not change the leading term. The coefficient at the leading term and next to the leading terms depend on particular function $f(z)$.

8 Numerical calculations

The contributions N_2 and N_3 to the normalization integral from the two- and three-body sectors are given by Eqs. (23) and (35) correspondingly. The difference:

$$N_{n\geq 4} = 1 - N_2 - N_3$$

is contribution to full normalization integral of higher Fock sectors (i.e., probability of the sectors with $n \geq 4$).

These probabilities, i.e., N_2, N_3 and $N_{n\geq 4}$ as function of M are shown in Fig. 10. Mass M (and momentum transfer Q below) are given in units of m, i.e., we put $m = 1$. The maximal values of N_3 and $N_{n\geq 4}$ are achieved at $M = 0$. In this case N_2 is calculated analytically by Eq. (26): $N_2 = 9/14 \approx 0.643$. N_3 is found numerically: $N_3 \approx 0.257$. Hence, the total contribution of the Fock sectors with $n \geq 4$: $N_{n\geq 4}(M = 0) = 1 - N_2 - N_3 = N_4 + N_5 + \ldots \approx 0.100$ is 10% only. Like in the case of form factor, this shows quick convergence relative to increase of the particle number in the Fock sectors. In the interval $0 \leq M \leq 1.8$ these contributions are rather smooth functions of M and then, when M tends to 2, N_2 tends to 1 and both N_3 and $N_{n\geq 4}$ tend to zero very quickly.

However, $N_{n\geq 4}$ decreases faster than N_3. This is seen from Fig. 11, where the ratio $\frac{N_{n\geq 4}}{N_3}$ vs. M is shown. This ratio decreases at $M \to 2$ and N_3 dominates over $N_{n\geq 4}$. This results from the fact that the higher Fock sectors $N_{n\geq 4}$ contain extra degree of α. This is also reflected in the coincidence of analytical formulas (25) for $N_{n\geq 3}$ with (37) for N_3.

In Fig. 12 the form factor $F_{full}(Q^2)$ is shown vs. Q^2 for the M values $M = 0$, 1.5, 1.9, 1.99, 1.9999. It is calculated by Eq. (39). We emphasize very strong dependence on M. For example, at $Q^2 = 1$ the form factor for $M = 1.9999$ is many orders ($\approx 10^6$ times) smaller than the form factor for $M = 0$.

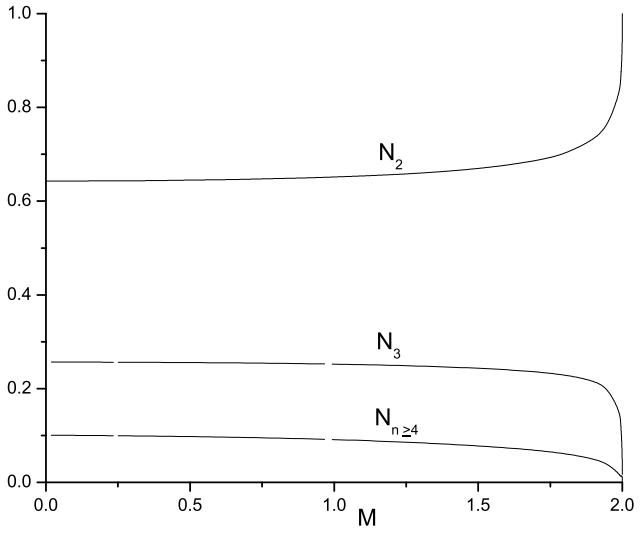

Fig. 10. Contribution to the full normalization integral of the states with the constituent numbers $n = 2$, $n = 3$ and $n \geq 4$.

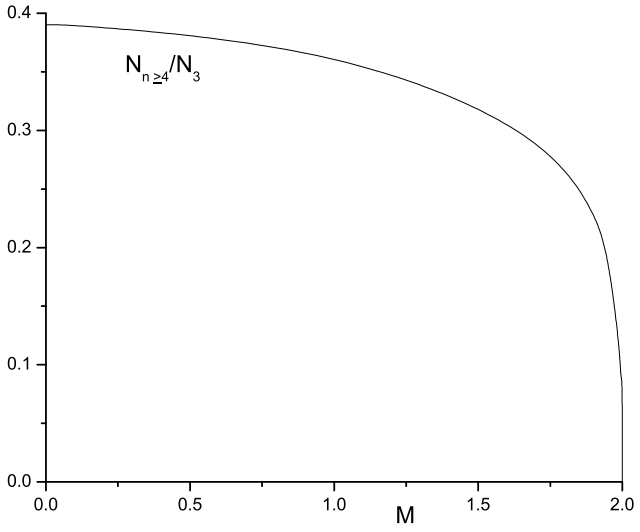

Fig. 11. Ratio $\frac{N_{n\geq 4}}{N_3}$ vs. M.

In order to show, how the two-body form factor achieves its asymptotic value, in Fig. 13 we present the ratios $F_{2b}^{asymp}(Q^2)/F_{2b}(Q^2)$ for $M = 0$ and $M = 1.9999$. For $M \to 2m$ the asymptotic form factor $F_{2b}^{asymp}(Q^2)$ is given by Eq. (28), and for $M = 0$ – by Eq. (31). We see that for small binding energy, $M = 1.9999$, the asymptotic is achieved much earlier (at $Q^2 \approx 0.1m^2$) than for large binding energy $M = 0$ ($Q^2 \approx 1000m^2$).

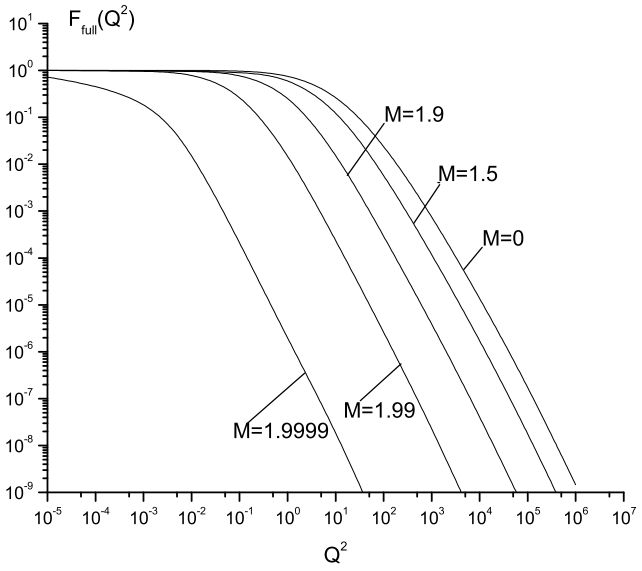

Fig. 12. Form factor $F_{full}(Q^2)$ vs. Q^2 for a few values of M.

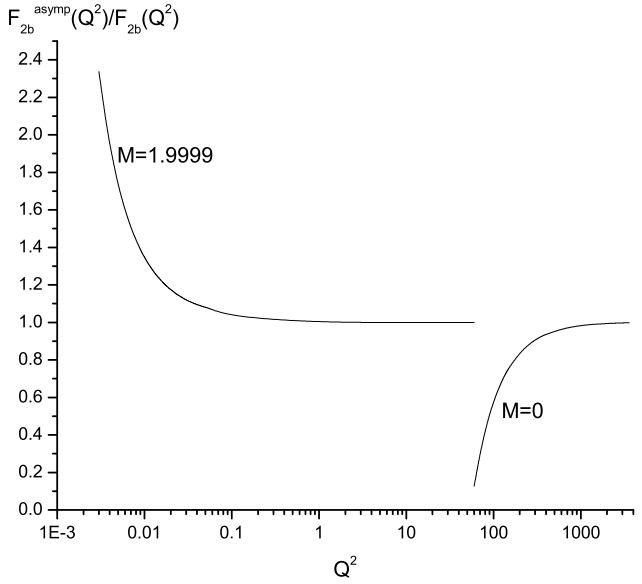

Fig. 13. Ratio of asymptotic of form factors $F_{2b}^{asymp}(Q^2)/F_{2b}(Q^2)$.

Similar situation takes place for the ratio of full form factors $F_{full}^{asymp}(Q^2)/F_{full}(Q^2)$. As shown in Section 5.3.2, at large values of Q^2 the many-body contribution decreases more rapidly than the two-body one. Therefore at $Q^2 \to \infty$ the form factor $F_{full}(Q^2)$ coincides with $F_{2b}(Q^2)$. The ratio of the form factors $F_{2b}(Q^2)/F_{full}(Q^2)$ vs. Q^2 for $M = 1.9999$ and $M = 0$ is shown in Fig. 14.

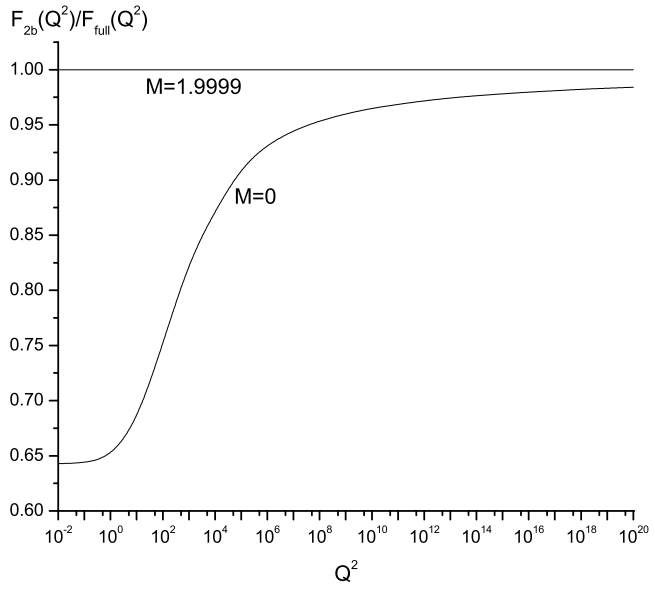

Fig. 14. Ratio of form factors $F_{2b}(Q^2)/F_{full}(Q^2)$.

For very small binding energy $B = 0.0001$ ($M = 1.9999$), and, correspondingly, small α, the many body contribution is practically absent. Therefore $F_{2b}(Q^2)/F_{full}(Q^2) \approx 1$ for any Q^2. For very large binding energy $B = 2$ ($M = 0$) the ratio $F_{2b}(Q^2)/F_{full}(Q^2)$ tends to 1, but it becomes more or less close to 1 at huge values $Q^2 \approx 10^{20} m^2$, when $\log(Q^2/m^2)$ dominates. Both form factors $F_{2b}(Q^2)$ and $F_{full}(Q^2)$ contain $\log(Q^2/m^2)$ with the same coefficient but they differ by the terms without $\log(Q^2/m^2)$ (the terms $-14/3 = -4\frac{2}{3}$ in $F_{2b}(Q^2)$ in (31) and -4 in $F_{full}(Q^2)$ in (41)). The difference of form factors is $-\frac{2}{3}$. Therefore the form factors $F_{2b}(Q^2)$ and $F_{full}(Q^2)$ become to be close to each other very far, when $\log(Q^2/m^2) \gg 2/3$. The relative difference $\Big(F_{full}(Q^2) - F_{2b}(Q^2)\Big)/F_{full}(Q^2)$ decreases as $\sim 1/\log(Q^2/m^2)$ only.

However, in a limited domain of Q^2 the form factors $F_{full}(Q^2)$ and $F_{2b}(Q^2)$ differ approximately by a factor. It is illustrated by Fig. 15 for $M = 1.5$. Solid line in this figure represents the form factor $F_{full}(Q^2)$. Dash line is $F_{2b}(Q^2)$. Its value at origin is: $N_2 = F_{2b}(0) = 0.669$ (compare with $N_2 = F_{2b}(0) = 9/14 = 0.643$ for $M = 0$). The dotted curve shows the two-body form factor $\tilde{F}_{2b}(Q^2) = F_{2b}(Q^2)/F_{2b}(0)$, normalized to 1 at $Q^2 = 0$. It is almost indistinguishable from $F_{full}(Q^2)$. If this coincidence takes place in a more realistic model, then, comparing the experimental data with the two-body form factor, normalized to 1 (as it is usually done), we would conclude that the later dominates and we would not notice 33% many-body contribution ($N_{n\geq 3} = 1 - 0.669 = 0.331$). This would be wrong conclusion about the structure of a system. Therefore the results shown in Fig. 15 could be instructive.

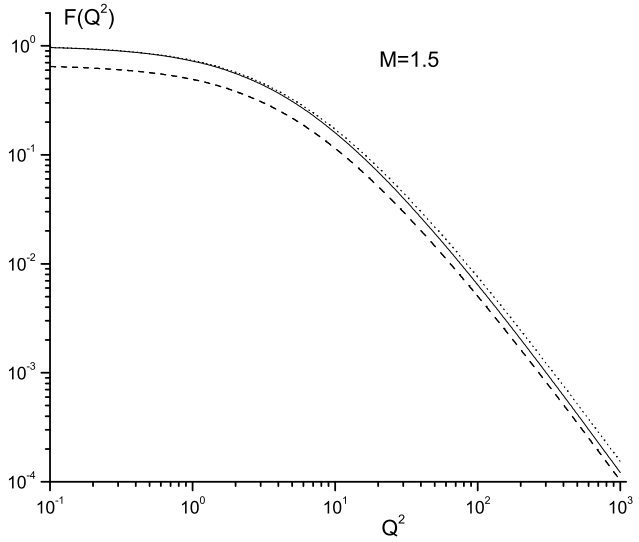

Fig. 15. Form factors for $M = 1.5$. Solid line – $F_{full}(Q^2)$. Dash line – $F_{2b}(Q^2)$. Dotted line – $\tilde{F}_{2b}(Q^2) = F_{2b}(Q^2)/F_{2b}(0)$.

9 Summary and discussion

The state vector in field theory does not correspond to a definite number of particles. It is represented as a superposition of Fock sectors with different particle numbers n. In Wick-Cutkosky model this sum starts with $n = 2$ and goes until infinity. We studied the contribution to the electromagnetic form factor (and, in particular, to the normalization integral) of the Fock sectors with $n = 2$, $n = 3$ and sum of all contributions with $2 \leq n < \infty$. For small and large binding energy (and coupling constant α) the results are obtained analytically (except for the three-body contribution at $M = 0$), and for arbitrary binding energy - numerically.

In the limit $\alpha \to 0$ the two-body sector survives only. Corresponding two-body Fock component is simply the non-relativistic ground state wave function in Coulomb potential.

In the next order $\sim \alpha \log \alpha$ the higher Fock sectors contribute, however the two-body sector still dominates. The correction $\sim \alpha \log \alpha$ comes from the three-body contribution, the correction $\sim \alpha^2$ results from many-body sectors with $n \geq 4$. Since at small α the higher Fock sectors are suppressed by extra degrees of α, the Fock decomposition converges very fast. Not only the normalization integral, but the form factor $F_{full}(Q^2)$, at any Q^2, is also dominated by the two-body contribution.

In the leading order $\alpha \log \alpha$ the contribution of many-body sectors to the nor-

malization integral $N_{n\geq 3}$, extracted from the BS function, Eq. (25), coincides with the three-body contribution N_3, Eq. (37), found by direct calculation in LFD of the three-body intermediate state. This coincidence illustrates the main idea of our work: the "two-body" BS function indeed includes many-body Fock sectors. Therefore both the two-body contribution N_2 and sum of many-body contributions $N_{n\geq 3}$ can be found from a given "two-body" BS function.

In the opposite case of large coupling constant, up to its maximal value $\alpha = 2\pi$ (corresponding to $M = 0$) the Fock decomposition still well converges. Contributions to the normalization integral of a few Fock sectors is presented in the Table 1. In spite of huge value of the coupling constant, contributions of the Fock sectors quickly decrease with increase of number of particles. Two first sectors with $n = 2$ and $n = 3$ determine 90% of the normalization integral.

N_2	N_3	$N_{n\geq 4}$	$N_2 + N_3 + N_{n\geq 4}$
0.643	0.257	0.100	1

Table 1
Contributions of the Fock sectors with the particle numbers $n = 2$, $n = 3$ and $n \geq 4$ ($N_{n\geq 4} = \sum_{n=4}^{\infty} N_n$) to the full normalization integral $N = \sum_{n=2}^{\infty} N_n = 1$ of the state vector for $M = 0$ ($\alpha = 2\pi$).

This can be explained as follows. Any extra Fock sector adds to the amplitude extra factor $\sim \alpha/(s - M^2)$. There is a competition between increasing coupling constant in numerator and increasing energy in denominator. When α increases, the binding energy increases too. Then the bound state mass M decreases. This results in increase of the energy denominators $(s - M^2)$ so that effective contribution of the factor $\sim \alpha/(s - M^2)$ remains smaller than 1. This is a probable mechanism of suppression of the higher Fock sectors in the Wick-Cutkosky model.

The behavior of form factors vs. Q^2 is also rather instructive. The decrease of full form factor $F_{full}(Q^2)$ (Fig. 12) with increase of Q^2 strongly depends on the bound state mass M. At smaller values of M the form factor begins to decrease at larger values of Q^2. At $M = 0$ the form factor is almost constant up to $Q^2 \approx 10m^2$ and decreases at larger Q^2.

Asymptotic of form factor for the larger binding energy B is achieved at larger values of Q^2 (Fig. 13). For mass $M = 1.9999$ form factor $F_{2b}(Q^2)$ obtains its asymptotic form at $Q^2 \geq m^2$, whereas for $M = 0$ – at $Q^2 \geq 1000m^2$.

The contribution of Fock sectors to form factor decreases with increase of Q^2 more faster for higher Fock sectors (for larger values of n). Therefore, in asymptotic only the two-body contribution survives (Fig. 14). For small

binding energy ($M = 1.9999$) the two-body component dominates for any Q^2. With increase of binding energy the many-body components become more important. However, they are suppressed at larger values of Q^2. The value of Q^2 when many-body contributions can be neglected is larger for larger binding energy. For $M = 0$ the many-body contributions become smaller than 5% (and the two-body form factor constitutes 95% of full form factor) at very large $Q^2 > 10^{10} m^2$.

The leading asymptotic terms $\sim \frac{1}{Q^4} \log \frac{Q^2}{m^2}$ in F_{full} and F_{2b} are the same (with the same coefficient). Therefore, at $Q^2 \to \infty$: $F_{full} = F_{2b}$. The form factor F_{3b} does not contain $\frac{1}{Q^4} \log \frac{Q^2}{m^2}$, but it contains next to the leading term $\sim \frac{1}{Q^4}$. With this correction F_{full} at $Q^2 \to \infty$ is determined by sum of two form factors, Eq. (42): $F_{full} = F_{2b} + F_{3b}$, where F_{3b} decreases faster than F_{2b}. Contributions $F_{n \geq 4}$ of the Fock sectors with $n \geq 4$ is the next correction which decrease faster than F_{3b}.

Though form factor F_{2b} substantially differs from F_{full}, in a limited but enough large domain of Q^2 their ratio is a constant. Being normalized at $Q^2 = 0$ to 1, $F_{2b}(Q^2)$ becomes to be very close to $F_{full}(Q^2)$ everywhere (see Fig. 15). Approximate description of true form factor of a system by the two-body one (with artificially imposed condition $F_{2b}(0) = 1$) does not mean that this system is the two-body one.

Good convergence of the Fock decomposition in Wick-Cutkosky model indicates that the Fock decomposition may be efficient in more realistic field theories, which, however, should be studied separately.

Acknowledgments

This work is supported in part by KISTEP (D.S.H.), and in part by the RFBR grant 02-02-16809 (V.A.K.).

A Correction $\sim \alpha \log \alpha$ to the Wick-Cutkosky solution

Eq. (11) with the kernel (12) is equivalent to the following differential equation:

$$g''_M(z) + \frac{\alpha}{\pi} \frac{m^2 g_M(z)}{(1 - z^2)\left[m^2 - \frac{1}{4}(1 - z^2)M^2\right]} = 0 \qquad \text{(A.1)}$$

with the boundary conditions $g_M(\pm 1) = 0$. In the limit $\alpha \to 0$ its solution (13) does not depend on α (except for a normalization factor). To find a correction to the Wick-Cutkosky solution (13), we solve Eq. (A.1), using the method of the paper [14]. Namely, the Eq. (A.1) is identically rewritten as:

$$g''_M(z) + \lambda(V_0 + V_1)g_M(z) = 0, \tag{A.2}$$

where

$$\lambda = \frac{\alpha}{\eta}, \quad \eta^2 = \frac{4m^2}{M^2} - 1, \quad V_0 = \delta(z), \quad V_1 = \frac{\eta}{\pi}\left[\frac{1+\eta^2}{(1-z^2)(\eta^2+z^2)}\right] - \delta(z).$$

Since the lowest order solution (13) $g^{(0)}(z) \equiv g_{M\to 2m}(z) \sim (1-|z|)$ is obtained from (A.2) at $V_1 = 0$, i.e., it satisfies the equation $g''^{(0)}(z) + \lambda^{(0)}V_0 g^{(0)}(z) = 0$ with $\lambda^{(0)} = 2$, V_1 can be considered as a perturbation. Eq. (A.2) becomes:

$$g''^{(0)} + g''^{(1)} + \ldots + (\lambda^{(0)} + \lambda^{(1)} + \ldots)(V_0 + V_1)(g^{(0)} + g^{(1)} + \ldots) = 0,$$

which in the first order gives [14]:

$$\lambda^{(1)} = \frac{-\lambda^{(0)} \int_{-1}^{1} g^{(0)} V_1 g^{(0)}\, \mathrm{d}z}{\int_{-1}^{1} g^{(0)} V_0 g^{(0)}\, \mathrm{d}z}$$

and the simple equation for $g^{(1)}$:

$$g''^{(1)} = -\left[\lambda^{(0)}V_0 g^{(1)} + \lambda^{(0)}V_1 g^{(0)} + \lambda^{(1)}V_0 g^{(0)}\right]. \tag{A.3}$$

From the relation $\lambda \equiv \lambda^{(0)} + \lambda^{(1)} = \frac{\alpha}{\eta}$ with $\lambda^{(0)} = 2$ we find the binding energy (16) and then the solution $g^{(1)}(z)$ of Eq. (A.3). It contains the terms $\sim \alpha$ and $\sim \alpha \log \alpha$. We have found that the next order correction $g^{(2)}(z)$ (relative to the order of the kernel V_1) contains the linear α contributions (i.e., the same order of α as appears in $g^{(1)}(z)$). But it does not contain the terms $\sim \alpha \log \alpha$. The binding energy calculated in [14] by another method (in LFD) coincides with (16) up to the $\sim \alpha \log \alpha$ terms too. Therefore we keep the leading $\sim \alpha \log \alpha$ term only. In this way we find eg. (15) for $g_M(z)$.

B Explicit BS solutions and the LF wave functions

Substituting (13) into (7), we find the BS function for asymptotically small binding energy explicitly:

$$\Phi_{M\to 2m}(k,p) = \frac{-4i\sqrt{2\pi}\alpha^{5/2}m^3}{\Big(m^2-\frac{1}{4}M^2-k^2-i0\Big)} \tag{B.1}$$

$$\times\frac{1}{\Big(m^2-(\frac{1}{2}p+k)^2-i0\Big)\Big(m^2-(\frac{1}{2}p-k)^2-i0\Big)}, \tag{B.2}$$

where $M = 2m - \frac{m\alpha^2}{4}$.

Substituting (18) into (7), we find the BS function for extremely large binding energy:

$$\Phi_{M=0}(k,p) = \frac{6i\sqrt{30}\pi m^3(k^2-m^2)}{(p{\cdot}k)^2\Big(m^2-k^2-p{\cdot}k-i0\Big)\Big(m^2-k^2+p{\cdot}k-i0\Big)}$$
$$-\frac{3i\sqrt{30}\pi m^3}{(p{\cdot}k)^3}\log\frac{m^2-k^2-p{\cdot}k-i0}{m^2-k^2+p{\cdot}k-i0}. \tag{B.3}$$

By means of Eq. (8) we find the LF wave functions for these two limiting cases:

$$\psi_{M\to 2m}(\vec{k}_\perp,x) = \frac{8\sqrt{2\pi}\alpha^{5/2}m^3x(1-x)}{\Big(\vec{k}_\perp^2+m^2-x(1-x)M^2\Big)^2}\times\begin{cases} x, & \text{if } 0\le x\le\frac{1}{2}\\ 1-x, & \text{if } \frac{1}{2}\le x\le 1\end{cases} \tag{B.4}$$

$$\psi_{M=0}(\vec{k}_\perp,x) = \frac{12\sqrt{30}\pi m^3x^2(1-x)^2}{\Big(\vec{k}_\perp^2+m^2\Big)^2}. \tag{B.5}$$

C Calculating form factors

C.1 Two-body form factor

To calculate the LF amplitudes, we use the Weinberg rules [11]. To find the amplitude $-\mathcal{M}$, one should put in correspondence: to every vertex – the factor g (in the theory with interaction $H^{int} = -g\varphi^2(x)\chi(x)$), to every intermediate state – the factor: $\frac{2}{s_0-s+i0}$, where s is the energy squared in the intermediate state, Eq. (3), and s_0 is the initial (=final) state energy. In our case (bound state): $s_0^2 = M^2$. To every internal line one should put in correspondence the factor: $\frac{\theta(x_i)}{2x_i}$. One should take into account the conservation laws for $\vec{R}_{i\perp}$ and x_i in any vertex and integrate over all independent variables with the measure: $\frac{\mathrm{d}^2R_{i\perp}\,\mathrm{d}x_i}{(2\pi)^3}$. The variables $\vec{R}_{i\perp}, x_i$ are introduced by Eq. (2) in Section 2.

The LF graph determining the EM vertex of two-body state is shown in Fig. 7. The energies squared corresponding to the intermediate states 1 and 2 in Fig. 7 read:

$$s_1 = (k_1 + k_2)^2 = \frac{\vec{R}_{1\perp}^2 + m^2}{x_1} + \frac{\vec{R}_{2\perp}^2 + m^2}{x_2} = \frac{\vec{R}_{1\perp}^2 + m^2}{x_1(1-x_1)},$$
$$s_2 = (k_1 + k_2')^2 = \frac{\vec{R'}_{1\perp}^2 + m^2}{x_1'(1-x_1')}. \tag{C.1}$$

We take into account: $R_1' \equiv k_1 - x_1 p' = R_1 - x_1 Q$, where $R_1 \equiv k_1 - x_1 p$ and $Q = p' - p$. Hence: $\vec{R'}_{1\perp} = \vec{R}_{1\perp} - x_1 \vec{Q}_\perp$. Using the rules [11], we get:

$$(p+p')_\rho \, F_{2b} = \int (k_2 + k_2')_\rho \, \Gamma' \, \frac{2}{M^2 - s'} \, \frac{2}{M^2 - s} \Gamma \times \frac{\theta(x_1)}{2x_1} \frac{\theta(x_2)}{2x_2} \, \frac{\theta(x_2)}{2x_2} \, \frac{\mathrm{d}^2 R_{1\perp} \, \mathrm{d}x_1}{(2\pi)^3}. \tag{C.2}$$

We used the standard condition $\omega{\cdot}Q = 0$. Therefore $\omega{\cdot}k_2 = \omega{\cdot}k_2'$ and, hence, $x_2' = x_2 = 1 - x_1$. Γ is the vertex function related to the wave function as:

$$\psi = \frac{\Gamma}{s - M^2}. \tag{C.3}$$

Multiplying both sides of the equality (C.2) by ω^ρ, we obtain the formula (20).

C.2 Three-body form factor and normalization integral

C.2.1 Form factor

We find form factor F_{3b}, calculating directly the amplitudes of diagrams Fig. 8. This is of course equivalent to perturbative calculation of the three-body component and then expressing form factor through it by a standard formula. Using the Weinberg rules [11], similarly to two-body contribution, Eq. (C.2), we obtain for the three-body graph Fig. 8 (a):

$$(p+p')_\rho \, F_{3b}^{(a)} = g^2 \int (k_4 + k_2')_\rho \times \Gamma' \, \frac{2}{(M^2 - s_4^{(a)})} \, \frac{2}{(M^2 - s_3^{(a)})} \, \frac{2}{(M^2 - s_2^{(a)})} \, \frac{2}{(M^2 - s_1^{(a)})} \, \Gamma \times \frac{\theta(x_1')}{2x_1'} \, \frac{\theta(1-x_1')}{2(1-x_1')} \, \frac{\theta(1-x_1')}{2(1-x_1')} \, \frac{\theta(x_1' - x_1)}{2(x_1' - x_1)}$$

$$\times \frac{\theta(x_1)}{2x_1}\,\frac{\theta(1-x_1)}{2(1-x_1)}\,\frac{\mathrm{d}^2R'_{1\perp}\,\mathrm{d}x'_1}{(2\pi)^3}\,\frac{\mathrm{d}^2R_{1\perp}\,\mathrm{d}x_1}{(2\pi)^3}. \qquad \text{(C.4)}$$

Here we used that $x_3 = x'_1 - x_1$, $x_4 = x'_2 = 1 - x'_1$, $x_2 = 1 - x_1$. The denominators $(M^2 - s_1^{(a)})$ and $(M^2 - s_4^{(a)})$ are absorbed in the relation (C.3) between Γ and ψ. The values of $s_2^{(a)}$, $s_3^{(a)}$ are defined in (33), (34). Multiplying both sides of Eq. (C.4) by ω^ρ, we obtain the contribution of graph Fig. 8 (a), which is half of Eq. (32).

Expression (33) for $s_2^{(a)}$ is found as follows. Since in the intermediate state 2 in the graph 8 (a) there are three particles (with the momenta k_1, k_3, k_4), according to Eq. (3) we have:

$$s_2^{(a)} = (k_1 + k_3 + k_4)^2 = \frac{\vec{R}^2_{1\perp} + m^2}{x_1} + \frac{\vec{R}^2_{3\perp}}{x_3} + \frac{\vec{R}^2_{4\perp} + m^2}{x_4},$$

where $\vec{R}_{1\perp}, \vec{R}_{3\perp}, \vec{R}_{4\perp}$ are the perpendicular to $\vec{\omega}$ components of the four-vectors

$$R_1 = k_1 - x_1 p, \quad R_3 = k_3 - x_3 p, \quad R_4 = k_4 - x_4 p.$$

Using the momenta conservation in the vertices, we transform R_3 as:

$$R_3 = k_3 - x_3 p = k'_1 - k_1 - (x'_1 - x_1)p \ \ (mod\ \ \omega) = R'_1 - R_1 + x'_1 Q,$$

where $(mod\ \ \omega)$ means that we omit the terms, proportional to ω since they do not contribute to the $\perp$-components. The variable R'_1 is defined as $R'_1 = k'_1 - x'_1 p'$. Hence we get: $\vec{R}_{3\perp} = \vec{R'}_{1\perp} - \vec{R}_{1\perp} + x'_1\vec{Q}_\perp$, as appears in (33). Similarly we find: $\vec{R}_{4\perp} = -\vec{R'}_{1\perp} - x'_1\vec{Q}_\perp$ and reproduce in this way Eq. (33) for $s_2^{(a)}$.

To find $s_3^{(a)}$, we start with:

$$s_3^{(a)} = (k_1 + k_3 + k'_2)^2 = \frac{\tilde{\vec{R}}^2_{1\perp} + m^2}{x_1} + \frac{\tilde{\vec{R}}^2_{3\perp}}{x_3} + \frac{\vec{R'}^2_{1\perp} + m^2}{x'_2},$$

where all R's are defined relative to p':

$$\tilde{R}_1 = k_1 - x_1 p', \quad \tilde{R}_3 = k_3 - x_3 p', \quad R'_1 = k'_1 - x'_1 p'$$

and then, again using the conservation laws, we find $\tilde{\vec{R}}_{1\perp} = \vec{R}_{1\perp} - x_1\vec{Q}_\perp$, $\tilde{\vec{R}}_{3\perp} = \vec{R'}_{1\perp} - \vec{R}_{1\perp} + x_1\vec{Q}_\perp$ and derive Eq. (34) for $s_3^{(a)}$.

Similarly we obtain the contribution of the diagram Fig. 8 (b):

$$F_{3b}^{(b)} = \frac{16\pi\alpha m^2}{(2\pi)^6} \int \frac{\psi(\vec{R}_{1\perp}, x_1)\ \psi(\vec{R'}_{1\perp}, x'_1)}{(s_2^{(b)} - M^2)(s_3^{(b)} - M^2)}$$

$$\times\frac{\theta(x_1-x_1')}{(x_1-x_1')}\frac{\mathrm{d}^2R_{1\perp}\,\mathrm{d}x_1}{2x_1(1-x_1)}\,\frac{\mathrm{d}^2R'_{1\perp}\,\mathrm{d}x_1'}{2x_1'(1-x_1')}, \tag{C.5}$$

where

$$s_2^{(b)}=\frac{(\vec{R'}_{1\perp}+x_1'\vec{Q}_\perp)^2+m^2}{x_1'}+\frac{(\vec{R}_{1\perp}-\vec{R'}_{1\perp}-x_1'\vec{Q}_\perp)^2}{x_1-x_1'}+\frac{\vec{R}_{1\perp}^2+m^2}{1-x_1}, \tag{C.6}$$

$$s_3^{(b)}=\frac{\vec{R'}_{1\perp}^{\,2}+m^2}{x_1'}+\frac{(\vec{R}_{1\perp}-\vec{R'}_{1\perp}-x_1\vec{Q}_\perp)^2}{x_1-x_1'}+\frac{(\vec{R}_{1\perp}-x_1\vec{Q}_\perp)^2+m^2}{1-x_1}. \tag{C.7}$$

By the replacement of variables $\vec{R}_{1\perp}\to\vec{R'}_{1\perp}, x_1\to x_1'$, $\vec{R'}_{1\perp}\to\vec{R}_{1\perp}, x_1'\to x_1$ we show that $F_{3b}^{(b)}=F_{3b}^{(a)}$. Therefore we finally get for full three-body contribution:

$$F_{3b}(Q^2)=F_{3b}^{(a)}(Q^2)+F_{3b}^{(b)}(Q^2)=2F_{3b}^{(a)}(Q^2)$$

and derive in this way Eq. (32) for $F_{3b}(Q^2)$.

C.2.2 Normalization integral

Three-body contribution to the normalization integral $N_3=F_{3b}(0)$ is given by Eq. (35). It is instructive to represent it through the interaction kernel. For this aim, we rewrite (35) as

$$\begin{aligned}N_3&=F_3^{(a)}(0)+F_3^{(b)}(0)\\&=\frac{\alpha m^2}{4\pi^5}\int\psi(\vec{R'}_{1\perp},x_1')\,\left[\frac{\theta(x_1'-x_1)}{(x_1'-x_1)(s_a-M^2)^2}+\frac{\theta(x_1-x_1')}{(x_1-x_1')(s_b-M^2)^2}\right]\\&\quad\times\psi(\vec{R}_{1\perp},x_1)\frac{\mathrm{d}^2R_{1\perp}\,\mathrm{d}x_1}{2x_1(1-x_1)}\,\frac{\mathrm{d}^2R'_{1\perp}\,\mathrm{d}x_1'}{2x_1'(1-x_1')}\end{aligned} \tag{C.8}$$

with

$$s_b=\frac{\vec{R'}_{1\perp}^{\,2}+m^2}{x_1'}+\frac{(\vec{R}_{1\perp}-\vec{R'}_{1\perp})^2}{x_1-x_1'}+\frac{\vec{R}_{1\perp}^2+m^2}{1-x_1}. \tag{C.9}$$

The ladder kernel is shown graphically in Fig. 16. Its calculation by the Weinberg rules [11] gives:

$$V=-\frac{4\pi\alpha\,\theta(x_1'-x_1)}{(x_1'-x_1)(s_a-M^2)}-\frac{4\pi\alpha\,\theta(x_1-x_1')}{(x_1-x_1')(s_b-M^2)}, \tag{C.10}$$

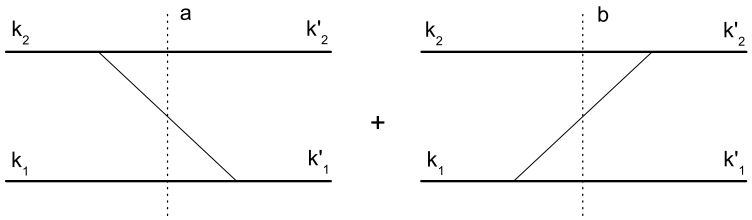

Fig. 16. Ladder kernel.

with s_a, s_b given by Eqs. (36), (C.9). The kernel (C.10) (which enters the Schrödinger-type equation) is related to the amplitude $\mathcal{K}$ of graph Fig. 16 as $V = -\mathcal{K}/(4m^2)$.

Let us calculate the derivative $\partial V/\partial M^2$:

$$\frac{\partial V}{\partial M^2} = -4\pi\alpha \left[\frac{\theta(x_1' - x_1)}{(x_1' - x_1)(s_a - M^2)^2} + \frac{\theta(x_1 - x_1')}{(x_1 - x_1')(s_b - M^2)^2}\right]. \qquad \text{(C.11)}$$

Comparing (C.11) with the integrand of (C.8), we represent N_3, Eq. (C.8), in the form

$$N_3 = -\frac{4m^2}{(2\pi)^6}\int \psi(\vec{R}'_{1\perp}, x_1')\ \frac{\partial V}{\partial M^2}\ \psi(\vec{R}_{1\perp}, x_1) \times \frac{\mathrm{d}^2 R_{1\perp}\,\mathrm{d}x_1}{2x_1(1-x_1)}\ \frac{\mathrm{d}^2 R'_{1\perp}\,\mathrm{d}x_1'}{2x_1'(1-x_1')}. \qquad \text{(C.12)}$$

Then we make replacement of variables $R_{1\perp}, x_1 \to k, \theta$:

$$R_{1\perp} = k\sin\theta, \quad x_1 = \frac{1}{2}\left(1 - \frac{k\cos\theta}{\varepsilon_k}\right), \qquad \text{(C.13)}$$

where $\varepsilon_k = \sqrt{k^2 + m^2}$, and similarly for $R'_{1\perp}, x_1' \to k', \theta'$. The integration volume is transformed as:

$$\frac{\mathrm{d}^2 R_{1\perp}\,\mathrm{d}x_1}{2x_1(1-x_1)} = \frac{R_{1\perp}\,\mathrm{d}R_{1\perp}\,\mathrm{d}x_1 d\phi}{2x_1(1-x_1)} = \frac{k^2 dk\sin\theta d\theta d\phi}{\varepsilon_k} = \frac{\mathrm{d}^3 k}{\varepsilon_k}.$$

In these variables N_3 obtains the form:

$$N_3 = -\frac{4m^2}{(2\pi)^6}\int \psi(\vec{k}', \vec{n})\ \frac{\partial V(\vec{k}', \vec{k}, \vec{n}, M^2)}{\partial M^2}\ \psi(\vec{k}, \vec{n})\ \frac{\mathrm{d}^3 k}{\varepsilon_k}\ \frac{\mathrm{d}^3 k'}{\varepsilon_{k'}}, \qquad \text{(C.14)}$$

where we introduced the vector $\vec{n}$: $\vec{k}\cdot\vec{n} = k\cos\theta$, $\vec{k}'\cdot\vec{n} = k'\cos\theta'$. The equation (C.14) coincides with the many-body contribution (for a general kernal V, not

only for the ladder one), given by Eq. (3.50) in [10]. It can be obtained by more general method [10], without precising the kernel V.

For small α the value N_3 can be calculated explicitly. We rewrite N_3, Eq. (35), as:

$$N_3 = \frac{\alpha m^2}{2\pi^5} \int \frac{\psi(\vec{R}_{1\perp}, x_1)\ \psi(\vec{R}'_{1\perp}, x'_1)(x'_1 - x_1)}{[(s_a - M^2)(x'_1 - x_1)]^2} \times\theta(x'_1 - x_1)\ \frac{\mathrm{d}^2 R_{1\perp}\,\mathrm{d}x_1}{2x_1(1-x_1)}\ \frac{\mathrm{d}^2 R'_{1\perp}\,\mathrm{d}x'_1}{2x'_1(1-x'_1)} \tag{C.15}$$

with s_a represented more explicitly:

$$s_a = \frac{\vec{R}^2_{1\perp} + m^2}{x_1} + \frac{R'^2_{1\perp} - 2R_{1\perp}R'_{1\perp}\cos\phi + R^2_{1\perp}}{x'_1 - x_1} + \frac{\vec{R}'^2_{1\perp} + m^2}{1 - x'_1}. \tag{C.16}$$

ϕ is angle between $\vec{R}_{1\perp}$ and $\vec{R}'_{1\perp}$. We make replacement of variables by Eqs. (C.13). Since N_3, Eq. (C.15), is proportional to α, for the wave function we can take Eq. (B.4) for asymptotically small α, where higher degrees of α are neglected. In the variables (C.13) it obtains the form (cf. Eq. (3.64) from [10]):

$$\psi(k,\theta) = \frac{8\sqrt{\pi m}\kappa^{5/2}}{(k^2+\kappa^2)^2\left(1 + \frac{k|\cos\theta|}{\sqrt{k^2+m^2}}\right)}, \tag{C.17}$$

where $\kappa = \sqrt{mB} = m\alpha/2$ (B is the binding energy).

Then we make another replacement of variables $k, k' \to p, p'$:

$$k = \kappa p, \quad k' = \kappa p', \tag{C.18}$$

where p, p' are dimensionless. In the limit $\kappa \to 0$, we decompose the factor $(s_a - M^2)(x'_1 - x_1)$ in the denominator of (C.15) in series of κ, keeping the leading term:

$$(s_a - M^2)(x'_1 - x_1) \approx \kappa^2 \Big[p^2 - 2pp'\cos\theta\cos\theta' - 2pp'\sin\theta\sin\theta'\cos\phi + p'^2 + \frac{\kappa}{m}(p^2 + p'^2 + 2)(p\cos\theta - p'\cos\theta')\Big] \tag{C.19}$$

Introducing vector $\vec{q} = \vec{p'} - \vec{p}$, we represent (C.19) as:

$$(s_a - M^2)(x'_1 - x_1) \approx \kappa^2(q^2 - \frac{\kappa}{m}(p^2 + p'^2 + 2)\vec{q}\cdot\vec{n}). \tag{C.20}$$

The difference $(x_1' - x_1)$ in the numerator of (C.15) is transformed as:

$$x_1' - x_1 \approx \frac{\kappa}{2m}(p\cos\theta - p'\cos\theta') = -\frac{\kappa}{2m}\vec{q}\cdot\vec{n}.$$

Wave function (C.17) obtains the form:

$$\psi(p) \approx \frac{8\sqrt{\pi m}\kappa^{5/2}}{\kappa^4(p^2+1)^2}. \tag{C.21}$$

It does not depend on θ, this simplifies the calculation. The integration volume reads:

$$\frac{\mathrm{d}^3k}{\sqrt{k^2+m^2}} \approx \frac{\kappa^3\,\mathrm{d}^3p}{m}.$$

Hence, N_3 is transformed as:

$$N_3 = -\frac{32\kappa m}{\pi^4}\int \frac{(\vec{n}\cdot\vec{q})\;\theta(-\vec{n}\cdot\vec{q})\;p^2dpdo_{\vec{p}}\;p'^2dp'do_{\vec{p'}}}{\left(mq^2-\kappa(p^2+p'^2+2)\;\vec{n}\cdot\vec{q}\right)^2(p^2+1)^2(p'^2+1)^2}. \tag{C.22}$$

One can substitute here denominator in the form of (C.19) and integrate over three angles θ, θ' and ϕ. However, the same result can be found in a more simple way. Namely, since N_3 in (C.22) does not depend on $\vec{n}$, but the integrand depends on $\vec{n}$, one can at first average integrand over the $\vec{n}$-directions. Therefore we replace the factor:

$$h_1 = \frac{(\vec{n}\cdot\vec{q})\;\theta(-\vec{n}\cdot\vec{q})}{\left(mq^2-\kappa(p^2+p'^2+2)\;\vec{n}\cdot\vec{q}\right)^2}$$

by

$$h_2 = \int \frac{(\vec{n}\cdot\vec{q})\;\theta(-\vec{n}\cdot\vec{q})}{\left(mq^2-\kappa(p^2+p'^2+2)\;\vec{n}\cdot\vec{q}\right)^2}\;\frac{do_{\vec{n}}}{4\pi}.$$

The angle integration here is one-dimensional and h_2 is easily calculated. After that the angle integrations in (C.22) are also carried out easily. Then the integrals over p and p' are calculated approximately, using that $\alpha \ll 1$ implies $\kappa \ll m$. In this way we obtain the analytical formula (37) for N_3 at $\alpha \ll 1$.

References

[1] E.E. Salpeter and H.A. Bethe, Phys. Rev. **84** (1951) 1232.

[2] G.C. Wick, Phys. Rev. **96** (1954) 1124;
R.E. Cutkosky, Phys. Rev. **96** (1954) 1135.

[3] N. Nakanishi, Prog. Theor. Phys. Suppl. **43** (1969) 1; **95** (1988) 1.

[4] R.J. Perry, A. Harindranath and K.G. Wilson, Phys. Rev. Lett. **65** (1990) 2959.

[5] N.C.J. Schoonderwoerd, B.J.L. Bakker and V.A. Karmanov, Phys. Rev. **C 58** (1998) 3093.

[6] J.R. Hiller and S.J. Brodsky, Phys. Rev. **D 59** (1999) 016006.

[7] D. Bernard, Th. Cousin, V.A. Karmanov and J.-F. Mathiot, Phys. Rev. **D 65** (2002) 025016.

[8] S.D. Glazek and R.J. Perry, Phys. Rev. **D 45** (1992) 3740.

[9] V.A. Karmanov, J.-F. Mathiot and A.V. Smirnov, Phys. Rev. **D 69** (2004) 045009.

[10] J. Carbonell, B. Desplanques, V.A. Karmanov and J.-F. Mathiot, Phys. Rept. **300** (1998) 215.

[11] S. Weinberg, Phys. Rev. **150** (1966) 1313.

[12] V.A. Karmanov, Nucl. Phys. **B 166** (1980) 378.

[13] M. Sawicki, Phys. Rev. **D 32** (1985) 2666; D 33 (1986) 1103.

[14] G. Feldman, T. Fulton and J. Townsend, Phys. Rev. **D 7** (1973) 1814.

[15] S.J. Brodsky, H. Pauli and S.S. Pinsky, Phys. Rept. 301 (1998) 299.

[16] G.P. Lepage and S.J. Brodsky, Phys. Rev. **D 22** (1980) 2157.

[17] S.J. Brodsky and D.S. Hwang, Nucl. Phys. **B 543** (1999) 239.

[18] S.J. Brodsky, D.S. Hwang, B. Ma and I. Schmidt, Nucl. Phys. **B 543** (1999) 239.

[19] S.J. Brodsky, J.R. Hiller D.S. Hwang and V.A. Karmanov, Phys. Rev. **D 69** (2004) 076001.

[20] V.A. Karmanov and A.V. Smirnov, Nucl. Phys. **A 546** (1992) 691.